

See discussions, stats, and author profiles for this publication at: <https://www.researchgate.net/publication/224931425>

Metal Ion-Enriched Polyelectrolyte Complexes and Their Utilization in Multilayer Assembly and Catalytic Nanocomposite Films

ARTICLE in LANGMUIR · MAY 2012

Impact Factor: 4.46 · DOI: 10.1021/la300674t · Source: PubMed

CITATIONS

12

READS

66

6 AUTHORS, INCLUDING:



[Md. Shahinul Islam](#)

Korea Basic Science Institute KBSI, Western S...

13 PUBLICATIONS 72 CITATIONS

[SEE PROFILE](#)



[Yong-Young Noh](#)

Dongguk University

220 PUBLICATIONS 4,011 CITATIONS

[SEE PROFILE](#)



[Ha-Jin Lee](#)

Korea Basic Science Institute KBSI

50 PUBLICATIONS 454 CITATIONS

[SEE PROFILE](#)

Metal Ion-Enriched Polyelectrolyte Complexes and Their Utilization in Multilayer Assembly and Catalytic Nanocomposite Films

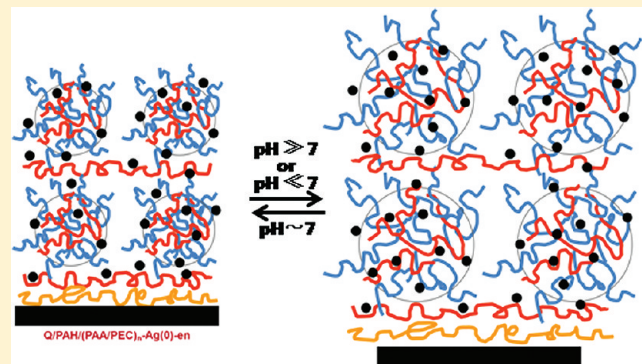
Md. Arifur Rahim,^{†,§} Md. Shahinul Islam,^{†,§} Tae Sung Bae,[†] Won San Choi,^{*,‡} Yong-Young Noh,[‡] and Ha-Jin Lee^{*,†}

[†]Jeonju Center, Korea Basic Science Institute (KBSI), 664-14 Dukjin-dong 1-ga, Dukjin-gu, Jeonju 561-756, Republic of Korea

[‡]Department of Chemical and Biological Engineering, Hanbat National University, San 16-1, Dukmyoung dong, Yuseong-gu, Daejeon 305-719, Republic of Korea

Supporting Information

ABSTRACT: The mixing of Ag ion-doped poly(ethyleneimine) (PEI) and poly(acrylic acid) (PAA) produced Ag ion-doped polyelectrolyte complex particles (PECs) in solution. Positively charged Ag ion-doped PECs (Ag ion PECs) with a spherical shape were deposited alternatively with PAA to form a multilayer assembly. The multilayered film containing Ag ion PECs was reduced to generate a composite nanostructure. Metal nanoparticle (NP)-enriched nanocomposite films were formed by an additional process of the postadsorption of precursors on PECs within the nanocomposite films, which resulted in the enhancement of the catalytic and electrical properties of the composite films. Because the films contain PECs that are responsive to changes in pH and most of the NPs are embedded in the PECs, interesting catalytic properties, which are unexpected in a particle-type catalyst, were observed upon pH changes. As a result of the reversible structural changes of the films and the immobilization of the NPs within the films, the film-type catalysts showed enhanced performance and stability during catalytic reactions under various pH conditions, compared to particle-type catalysts.



INTRODUCTION

The layer-by-layer (LbL) self-assembly technique using polyelectrolytes (PEs) has been proven to be a simple and inexpensive way to fabricate various types of nanocomposites with a tailored chemical composition.^{1–10} The LbL assembly technique holds great promise in the fabrication of nanocomposites for the following reasons: first, a wide range of materials can be easily incorporated into nanocomposites; second, the LbL assembly technique enables the deposition of nanomaterials on flat and nonflat surfaces with large areas; third, the LbL assembly technique allows the precise control necessary to form films with nanometer-scale thickness. For PE-based nanocomposites, the incorporation of inorganic materials into the PE structures is necessary. Metal nanoparticle (NP)-embedded polyelectrolyte multilayer (PEM) thin films have been proven to be more feasible than other forms of nanocomposites. For the incorporation of NPs into PEMs, the *in situ* reduction method has generally been used.^{11,12} The loading of metal precursors and their successive reduction in PEMs form the principle steps of this method.^{11–13} Recently, metal-loaded thick PEM films were reported to show an interesting property that is not achieved in metal-loaded thin PEM films.¹⁴ However, because the conventional LbL method uses PEs only as building blocks, preparing thick films is time-consuming and ineffective as a result of numerous tedious

processes. Therefore, nanocomposite films highly loaded with metal NPs are difficult to obtain.

Mixing PEs of opposite charge in a nonstoichiometric ratio can cause several hundred nanometer-sized PE complexes (PECs) that are stable in an aqueous solution to form.^{15,16} The use of PECs as a building block for multilayer assembly has recently been reported.^{17,18} The utilization of PECs for the preparation of multilayer films has some advantages over a conventional LbL assembly with common PEs. The high thickness and tunable properties of the composite films can be easily achieved within a few layers of deposition. The advantages of the PEC-based systems could enable the formation of a nanocomposite with controlled properties that is heavily loaded with metal NPs for various practical applications. Thus, the development of novel fabrication methods for such PEC-based systems is necessary and has much potential.

In this study, a novel fabrication technique for conductive and catalytic nanocomposite films with highly embedded metal NPs was demonstrated using silver-doped PECs. Before PECs are formed, Ag precursors were preadsorbed on poly-

Received: February 16, 2012

Revised: May 8, 2012

Published: May 9, 2012

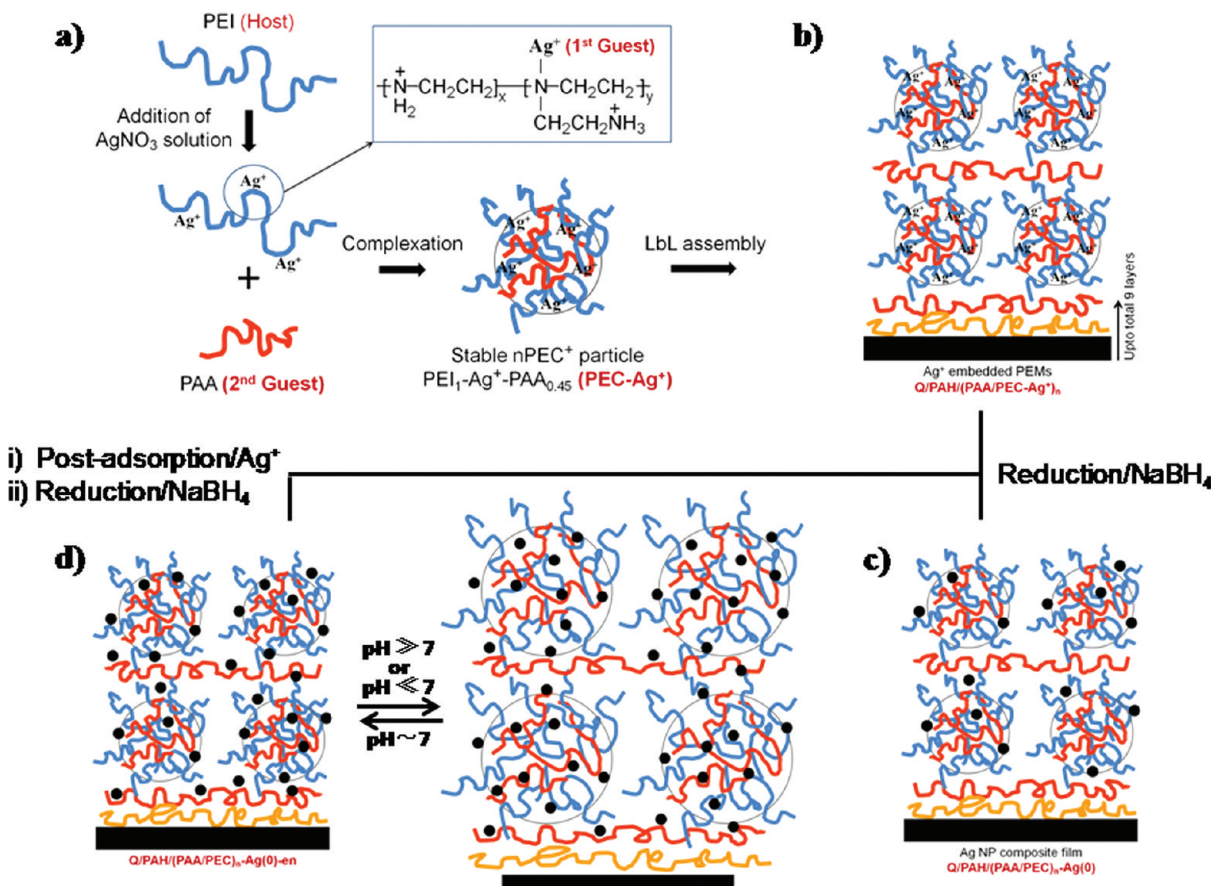


Figure 1. Schematic representation of the fabrication process of the PEC-Ag⁺ particles and structural changes of the highly loaded AgNP-containing composite film prepared via pre- and postadsorption.

(ethyleneimine) (PEI) for the homogeneous synthesis and high loading of metal NPs within PECs. The successive mixing of poly(acrylic acid) (PAA) in PEI-Ag⁺ solution forms positively charged Ag ion-doped PEC particles (PEI-Ag⁺/PAA). These particles were alternatively assembled with PAA to form a multilayer film. Finally, the chemical reduction of the pristine film and an additional loading step of metal precursors produced PEC-AgNP nanocomposite films with densely loaded NPs. The goal of our study is to synthesize a metal NP-enriched composite film and reversibly control the film structure as well as the distribution of the NPs within the film by external stimuli. Moreover, the possibility of a film-type catalyst showing reversible and stable catalytic properties without catalyst damage or performance deterioration was demonstrated for the first time. What clearly distinguishes this method from those previously reported is as follows: (i) To the best of our knowledge, the method we used here to synthesize metal NP-enriched polymer particles through a combination of pre- and postadsorption has not yet been reported, which is also able to tune the content of AgNP's precisely within the PECs. Moreover, the combination adsorption of metal precursors on PECs within the nanocomposite films can produce metal NP-enriched nanocomposite films with enhanced catalytic and electrical properties. In the previous studies, the metal ions were embedded after completing the PEC or multilayer formation, which is not effective for preparing a metal NP-enriched matrix with good dispersibility. (ii) The use of PECs enables the facile fabrication of thick films with minimal effort in terms of the number of layers. (iii) A

film-type catalyst, which undergoes a catalytic reaction under various pH conditions without film damage or performance deterioration and can be easily collected after the catalytic reaction, is used. Our research demonstrates the possibility of both a simple process for preparing composite films heavily loaded with metal NPs and a real application for film-type catalysts.

EXPERIMENTAL SECTION

Materials. Poly(ethylene imine) (PEI, $M_w = 25\,000$), poly(acrylic acid) (PAA, $M_w = 1800$ and $450\,000$), silver nitrate (AgNO_3 , 99.99%), sodium borohydride (NaBH_4), and 4-nitrophenol were purchased from Sigma-Aldrich and used as received. Deionized water (Millipore) was used for all experiments.

Preparation of PEI-Ag⁺/PAA_{0.45} Complexes Particles: PEC-Ag⁺. The PEI-Ag⁺ complexes were prepared by dropping an aqueous AgNO_3 solution (5 mM, 5 mL) into 10 mL of an aqueous PEI solution (0.9 mg/mL) under moderate stirring at 450 rpm. After 15 min, 10 mL of an aqueous PAA solution (0.7 mg/mL) was added to the PEI-Ag⁺ complex solution at the same stirring rate. The final mixture was further stirred for 15 min to obtain the final complex particles, PEI-Ag⁺/PAA_{0.45}. The feed monomer molar ratio of PEI to PAA was 1:0.45, and the pH of the final dispersion was 6.7.

Film Preparation: Q/PAH/(PAA/PEC-Ag⁺)_n. A quartz plate was cleaned in a piranha solution (1:3 30% H_2O_2 /98% H_2SO_4) and heated until no bubbles were released. (**Caution!** Piranha solution reacts violently with organic material and should be handled carefully.) The cleaned quartz substrate was primed with a PAH layer by dipping the substrate into a PAH solution (2 mg/mL, pH 9) for 15 min and rinsed in DI water (adjusted pH to 9) twice. Next, the PAH-coated substrate was dipped into a PAA solution (1 mg/mL, $M_w = 450\,000$), rinsed

twice with DI water, and dried in a stream of N_2 . The resulting PAA-terminated substrate was then immersed in the PEC ($PEI_1\text{-Ag}^+$ /PAA_{0.45}) complex solution for 15 min, rinsed twice, and dried in a stream of N_2 . The last two procedural steps were repeated until the desired number of layers was obtained.

Preparation of Composite Films: Q/PAH/(PAA/PEC)_n-Ag(0). The desired composite film was prepared by reducing a Q/PAH/(PAA/PEC)_n multilayer film using an aqueous NaBH₄ solution (5 mM) for 30 min. To enrich the Ag NP content of the composite film, the Q/PAH/(PAA/PEC)_n multilayer film was immersed in a AgNO₃ (5 mM) solution for 10 min and then reduced in a NaBH₄ solution (5 mM).

Catalytic Reduction of 4-Nitrophenol. The catalytic reduction of 4-nitrophenol by NaBH₄ in the presence of both composite films, Q/PAH/(PAA/PEC)₄-Ag(0) and Q/PAH/(PAA/PEC)₄-Ag(0)-en, was studied by UV-vis absorption spectroscopy. The reaction was performed in a UV quartz cuvette ($1 \times 1 \text{ cm}^2$). In a typical experiment, a 4-nitrophenol solution (0.15 mM, 0.3 mL) was mixed with a NaBH₄ solution (5 mM, 2.5 mL) in a quartz cuvette. After the corresponding composite film was immersed in the 4-nitrophenol solution, the absorption spectra were recorded at 7 min intervals in the spectral range of 200–600 nm at room temperature.

Characterization. Dynamic light scattering (DLS) studies and ζ -potential measurements were performed on a Malvern Nano-ZS zeta sizer at room temperature. UV-vis absorption spectra were recorded on a UV-vis-NIR spectrophotometer (Shimadzu UV-3600). Atomic force microscopy (AFM) measurements were performed using a Nanoscope IV multimode AFM (Veeco). XPS studies were performed on an Axis NOVA (Kratos Analytical) spectrometer using an aluminum anode (Al KR 1486.6 eV) operated at 600 W. UHR-SEM micrographs were obtained using a Hitachi S-5500 instrument. For the FESEM measurement, the composite film was peeled off of the quartz substrate with hydrofluoric acid (HF), allowed to float in water, and then collected on a carbon-coated copper grid.¹⁹ Conductivity measurements of the Q/PAH/(PAA/PEC)₄-Ag(0), Q/PAH/(PAA/PEC)₄-Ag(0)-en, and Q/PAH/(PAA/PEI-Ag(0))₁₇ films were carried out on an MST 4000A test unit using a four-point probe head with a pin distance of about 1 mm.

RESULTS AND DISCUSSION

Figure 1 shows a schematic for the preparation of PEC-Ag⁺ and its nanocomposite films. PEI functioned as a cationic host material, and a silver precursor (Ag⁺) and PAA were used as the first and second guest materials, respectively. PEI is known to be an effective compound for forming complexes with metal precursors^{20,21} because the tertiary amine groups in PEI are capable of forming complexes with metal ions.²⁰ Because Ag⁺ usually binds to the tertiary groups of PEI, the secondary and the primary amine groups of PEI remain available for further complexation with other suitable materials (PAA in this study). PEI was first complexed with Ag⁺ in solution, and then the PEI-Ag⁺ complex was further complexed with PAA in a non-stoichiometric mixing ratio. After the successive complexation process, the product (PEI₁-Ag⁺-PAA_{0.45}, subscripts are the ratio of the monomeric units of PEI and PAA, 1:0.45, respectively), was formed, which will be denoted throughout the text as PEC-Ag⁺ particles. Because an excessive amount of the PEI-Ag⁺ complex is formed in the solution (in terms of PEI monomeric units) compared to PAA, the final PEC-Ag⁺ particles are rendered a net positive charge (Figure 1a). Next, the PEC-Ag⁺ particles were alternatively assembled with PAA to construct a multilayer film having the required number of layers (Figure 1b). It should be noted that the quartz substrate was primed with a PAH layer before forming the multilayer film. Finally, the multilayer film was reduced to create a silver nanoparticle (AgNP) composite film (Figure 1c). The pristine film in which

Ag⁺ is not reduced is denoted as Q/PAH/(PAA/PEC-Ag⁺)_n, whereas the final composite film containing AgNP after reduction is denoted as Q/PAH/(PAA/PEC)_n-Ag(0). To produce a AgNP-enriched composite film, an external loading step was performed on the Ag precursor-embedded films (Q/PAH/(PAA/PEC-Ag⁺)_n) for additional adsorption of Ag precursors (Figure 1d). The resulting composite films underwent structural changes at low or high pH owing to the presence of PEC particles.

The PEC-Ag⁺ particles in solution were characterized using dynamic light scattering (DLS) and zeta potential techniques. Their average particle size was found to be 212 nm (Figure 2a).

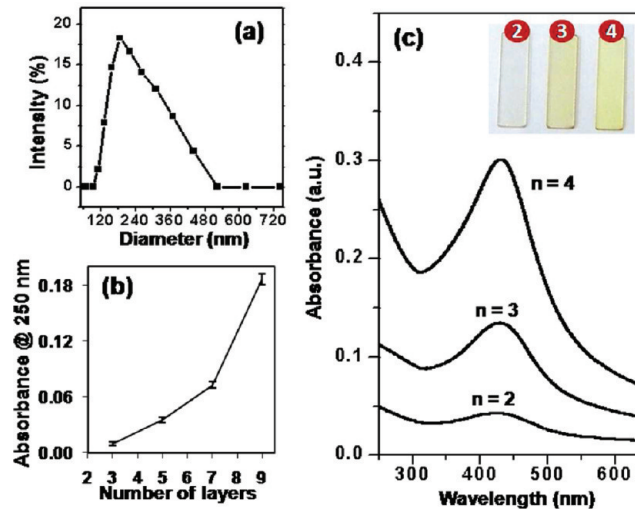


Figure 2. (a) Particle size distribution of the PEC-Ag⁺ particles measured by DLS, (b) nonlinear growth pattern of the composite film [Q/PAH/(PAA/PEC-Ag⁺)₃] prepared during multilayer formation, and (c) UV-vis absorption spectra of the composite films after reduction, Q/PAH/(PAA/PEC)_n-Ag(0) ($n = 2-4$). The corresponding images of the films with different layers are displayed in the inset.

Moreover, the absence of particles that were less than 50 nm in size confirms the absence of any free PE in the dispersion because the hydrodynamic diameter of PEI ($M_w = 25\,000$) is 11 nm.²² The absence of free PEs (PEI or PAA) in the PEC-Ag⁺ particle solution was further confirmed by the following test.²³ The PEC-Ag⁺ solution was filtered to separate the PEC-Ag⁺ particles, and a clear supernatant solution was obtained. Half of the supernatant was reacted with the polyanion, PSS, and the other half was reacted with the polycation, PAH. The solution was expected to be turbid if free PEs were present; however, no turbidity was observed for either solution (Figure S1), proving that no free PEs remained in the solution and all PEs were consumed to form PEC-Ag⁺ particles. As expected, the zeta potential of the PEC-Ag⁺ particles suggested that the particles were +62 mV, which is a positive charge (Figure S2).

The layer growth of the multilayer buildup was monitored using UV-vis absorption spectroscopy. The overall absorbance increased with an increasing number of layers as a result of the thickness increment of the films (Figure S3), which is in accordance with previously reported results,²⁴ suggesting the successful growth of multilayers consisting of PAA and PEC-Ag⁺ particles. We prepared nine layered multilayers and observed that the multilayers showed nonlinear growth behavior within the range of investigation (Figure 2b). Higher deposition occurred with increasing layer number (seventh-

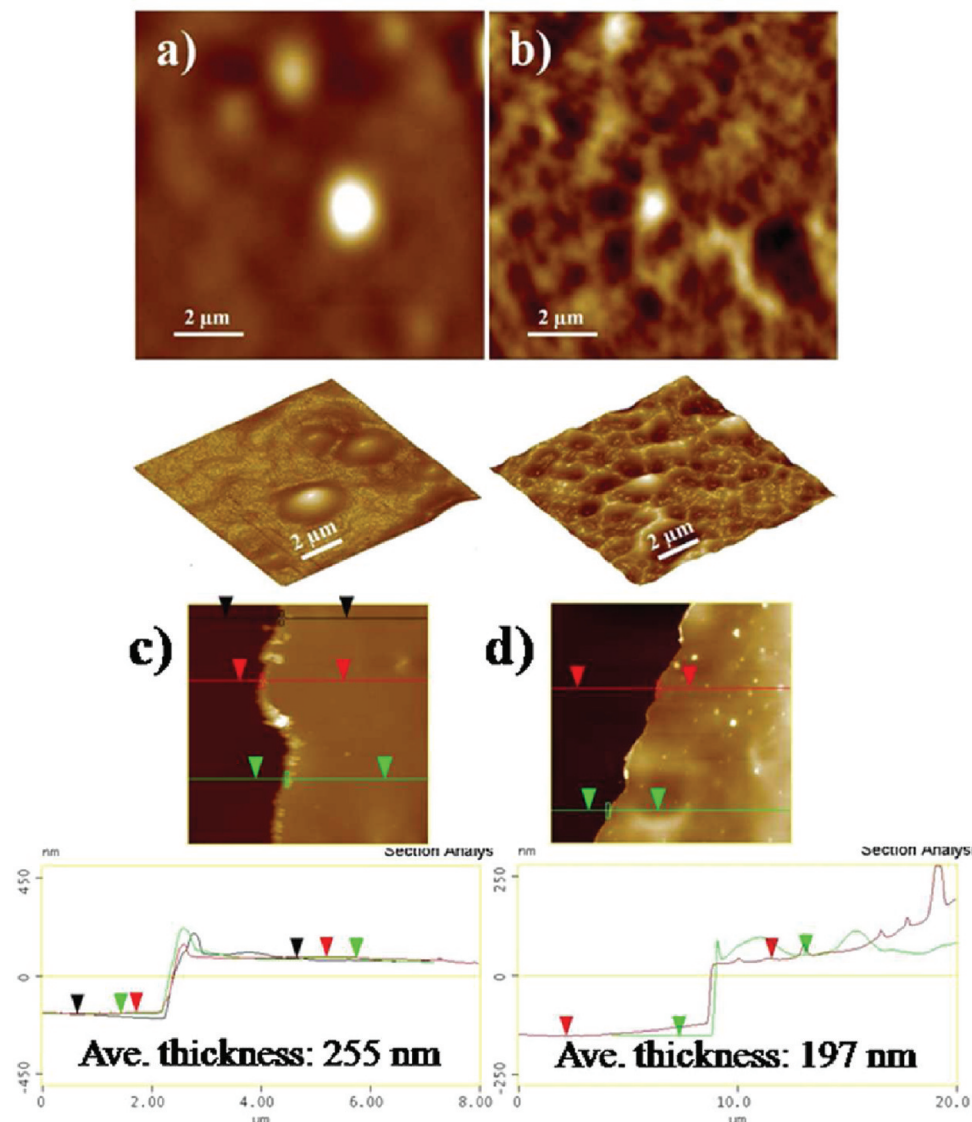


Figure 3. AFM surface topographies of the Q/PAH/(PAA/PEC)₄ film (a) before and (b) after reduction. The lower panels show the corresponding 3D morphologies of the films. Topologies and height profiles of (c) the Q/PAH/(PAA/PEC)₄ and (d) the Q/PAH/(PAA/PEC)₄-Ag(0) films prepared by the scratching-off method.

ninth layers), probably owing to the influence of the substrate surface charge in the initial bulid-up regime (alternatively termed the nonlinear regime), which is in consistent with previous observations.^{17,18} It should be noted that a linear growth regime is also probable for multilayers with a large number of layers. After the chemical reduction of Q/PAH/(PAA/PEC-Ag⁺)₄, the color changed from transparent to light yellow, which suggested the formation of AgNP's within the film (Q/PAH/(PAA/PEC)₄-Ag(0)). Figure 2c shows UV-vis absorbance spectra of the composite film, Q/PAH/(PAA/PEC)_n-Ag(0), as a function of the number of layers. The corresponding photographs of the composite films are shown in the inset of Figure 2c. A strong surface plasmon resonance (SPR) is shown in the range of 400–450 nm as a result of the collective oscillation of the free conduction electrons, which is commonly observed in metal NPs such as Au and Ag.²⁵ Typically, a single, intense absorption peak in the visible region is exhibited by spherical metal NPs with diameters of less than 100 nm.²⁶ In the present case, all of the composite films showed an absorption peak at approximately 428 nm, and the

peak intensity increased with the increasing number of layers. The slight variation (1–3 nm) in the absorbance maxima (λ_{\max}) of the films can be attributed to the subtle change in refractive indices with the different number of layers.^{27,28} The differences in the absorption intensities of AgNP's for the different number of layers is indicative of the nonlinear growth behavior of the multilayer film, as shown in Figure 2b.

Figure 3 shows the surface morphologies observed using atomic force microscopy (AFM) on the pristine films before and after the synthesis of AgNP's. Using the scratching method, the thickness of the pristine film was measured to be 255 nm. An average PEC-Ag⁺ particle size of 212 nm translates to a film thickness of approximately 1 μm for four PEC-Ag⁺ particle layers. However, the observed thickness had a much lower value (255 nm), which resulted from the deformation and squeezing of the PEC-Ag⁺ particles during the multilayer formation and drying process. Similar behavior was observed in a multilayer assembly using PEC particles.^{29,30} After a reduction of the Ag precursors, AgNP-embedded composite films (Q/PAH/(PAA/PEC)_n-Ag(0)) had a thickness of 197 nm, which

was decreased from 255 nm. Moreover, the surface roughness of the films increased compared to that of the pristine films. The rms roughness values of the pristine and composite films were determined to be 7.56 and 11.79 nm, respectively. The decrease in thickness and the increase in roughness of the composite film can be explained by the further rearrangement of the components in the multilayer film during the reduction process. Overview SEM images clearly demonstrate the success of the proposed approach over a large area (Figure S4).

Chemical binding states and characteristics of the composite film were investigated using XPS measurements. As displayed in the survey spectrum, C 1s, O 1s, N 1s, and Ag 3d peaks were detected, which is consistent with the composite film compositions (Figure 4a). From the C 1s core-level photo-

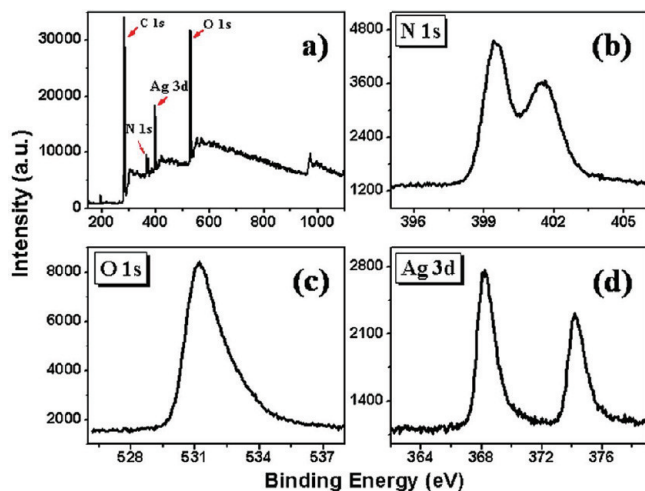


Figure 4. XPS spectra of the composite film [Q/PAH/(PAA/PEC)₄-Ag(0)]. (a) Survey spectra, (b) N 1s core-level spectrum, (c) O 1s core-level spectrum, and (d) Ag 3d core-level spectrum.

electron spectrum, the binding energy was observed to occur at 285 eV, with a shoulder peak at approximately 287 eV (Figure S5). The deconvoluted C 1s spectrum showed two distinct spectral features, which resulted from different carbon species in the film. The major peak observed at 285.7 eV can be attributed to the presence of hydrocarbon groups.³¹ The shoulder peak at 287.8 eV can be attributed to the carbonyl group (C=O) in PAA.³² The N 1s signal originating from PEI had two peaks positioned at 399.5 and 401.5 eV (Figure 4b). The former and the latter can be attributed to the unprotonated amine groups and the protonated amine groups, respectively.^{33,34} This feature indicates the presence of different amine groups in PEI. Unlike C 1s and N 1s, a single peak at 531.2 eV for O 1s was observed and is regarded to be the carboxylic acid group (COO⁻) in PAA (Figure 4c).^{35,36} The chemical state of the Ag species in the composite films can be determined from the Ag 3d_{5/2-3/2} core-level spectrum (Figure 4d). The Ag components in the composite film were completely reduced to their elemental state, as confirmed by the appearance of doublet peaks from elemental Ag located at 368.2 and 374.2 eV, with a spin-orbit separation of 6 eV.³³ Considering the area under each curve and applying the standard sensitivity factors for each element, we determined the atomic composition of the film to be C (53.3%), O (22.6%), N (22%), and Ag (2.1%). These observed quantitative values are in accordance with the theoretical quantities of our experimental procedure. For example, according to the mixing

ratio of PEI and Ag⁺ based on the molar concentration of the PEI-Ag⁺ complex solution, the theoretical number of Ag atoms was determined to be ~11.5% of the number of N atoms in PEI. Meanwhile, the atomic composition of the Ag atoms observed from the XPS spectra was calculated to be ~10.45% of the number of N atoms in PEI in the composite films. This result also indicates nearly complete coordination and retention of the Ag⁺ ions in the PEIs during the initial PEC-Ag⁺ particle formation and the multilayer buildup, respectively. Again, considering the PEC-Ag⁺ particle theoretically, the molar ratio of the N atoms in PEI and the O atoms in PAA was 1:0.9 (monomeric mixing ratio of 1:0.45, where there exists 1 N atom from PEI and 2 O atoms from PAA). From the XPS result, the ratio was calculated to be 1:1.02, which is in accordance with the theoretical atomic composition ratio.

Figure 5a,b shows ultrahigh-resolution field-emission scanning electron microscope (UHR-FESEM) images of the composite film. Black spots indicating AgNP's are apparent in the film and have a dense population. The particles were observed to be polydisperse and well distributed in the film. The corresponding EDX analysis also confirmed the existence of Ag in the film (Figure 5c). One hundred AgNP's were randomly selected from the image and had their particle size measured. The particle size distribution is shown in the histogram, and its mean size was calculated to be ~5.5 nm (Figure 5d).

The number of AgNP's within the films could be increased remarkably by the postadsorption of the silver precursor on the films. Prior to the reduction of Q/PAH/(PAA/PEC-Ag⁺)₄, the as-prepared pristine film was dipped into a AgNO₃ solution and subsequently reduced using NaBH₄. That process is schematically displayed in Figure 1. The AgNP-enriched composite film, Q/PAH/(PAA/PEC)₄-Ag(0)-en, exhibited a much higher absorption intensity than did the Q/PAH/(PAA/PEC)₄-Ag(0) composite film (Figure 6a,c), which implies further incorporation of AgNP's into the film after postadsorption. The enrichment of the AgNP's can be explained in the following manner. The initial Ag⁺-doped PEC particles (PEC-Ag⁺) were assembled alternatively with PAA in the multilayer film. When this pristine film was immersed in a AgNO₃ solution, the protonated carboxylic groups of PAA, acting as an anionic layer, provided available reaction sites where the ion exchange of Ag⁺ can take place.¹² Moreover, the PEC-Ag⁺ particles underwent a structural change during the assembly of the multilayer film, as suggested from the decrease in thickness using AFM. Thus, the PAA present with the PEC-Ag⁺ particles provided more reaction sites for the Ag precursors. The successful enrichment of the AgNP's in the composite films is also apparent by the increased peak intensity of the Ag 3d core-level spectrum observed in the XPS analysis (Figures 4d and 6b). UV-vis absorbance at λ_{max} also showed an increase of ~94% (Figure 6c, left panel), and XPS showed an enhancement of ~58% with a total Ag content of 3.17% (atomic %) in the film (Figure 6c, right panel). Moreover, the film color became darker for the enriched film (inset of Figure 6a).

For a more exact evaluation of the advantage of the composite films, a 35-layer PE multilayer film, Q/PAH/(PAA/PEI-Ag⁺)₁₇, that was composed of PAA and PEI-Ag⁺ on a quartz substrate primed with PAH was prepared and used for the enrichment of the AgNP's in the films. The 35-layer PE multilayer film containing Ag precursors was prepared by a conventional layer-by-layer method without PEC-Ag⁺ particles, and the average film thickness (208 nm) was nearly identical to

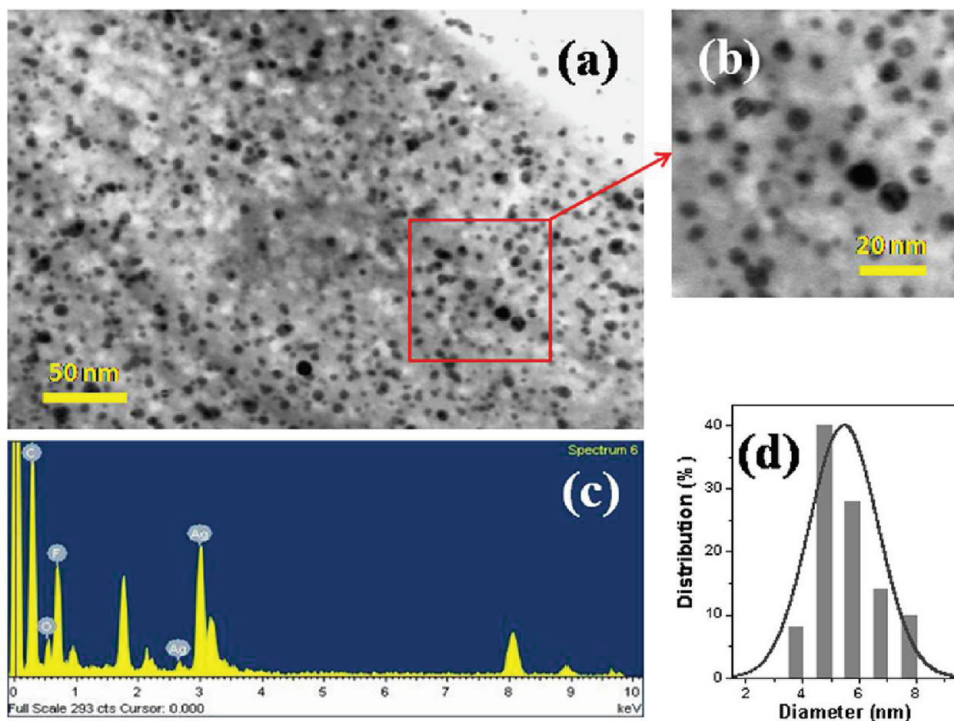


Figure 5. (a, b) UHR-FESEM micrographs of the Q/PAH/(PAA/PEC)₄-Ag(0) composite film. (b) Selected magnified image of part a. (c) EDX analysis of the composite film showing the presence of Ag. (d) Size distribution of AgNP's calculated from the UHR-FESEM micrographs.

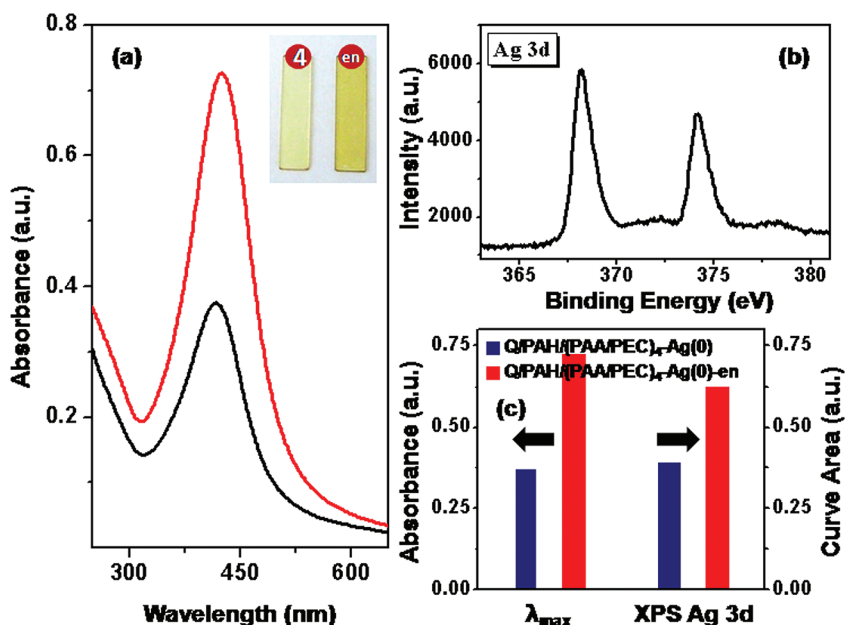


Figure 6. (a) UV-vis absorption spectra of the composite films, Q/PAH/(PAA/PEC)₄-Ag(0) (black line) and Q/PAH/(PAA/PEC)₄-Ag(0)-en (red line). Visual color differences in the two films are shown in the inset. Q/PAH/(PAA/PEC)₄-Ag(0) is marked as 4, and Q/PAH/(PAA/PEC)₄-Ag(0)-en is marked as en. (b) XPS data showing the Ag 3d core-level spectrum of the enriched film. (c) The absorbance (left panel) and Ag 3d (XPS Ag 3d) intensity (right panel) are compared for films Q/PAH/(PAA/PEC)₄-Ag(0) (blue bar) and Q/PAH/(PAA/PEC)₄-Ag(0)-en (red bar).

that of Q/PAH/(PAA/PEC-Ag⁺)₄. The film showed a gradual growth of multilayers as a function of the increasing number of layers (Figure 7a). After reduction, a single absorption peak from the AgNP's was observed at approximately 425 nm (black line, Figure 7b). The peak intensity further increased after the Ag enrichment process (red line). However, its intensity increased by only 11% of the initial absorbance of the Q/PAH/(PAA/PEC-Ag(0))₁₇ films, which is minimal compared to the

94% increase in the case of the Q/PAH/(PAA/PEC)₄-Ag(0)-en films. In summary, the loading rate of the Q/PAH/(PAA/PEI-Ag(0))₁₇ films during the enrichment process was unimpressive even though these films were thick enough. These results mean that the content of AgNP's within the films can be increased remarkably by one simple dipping if the PEC-Ag⁺ particles are used for multilayer buildup.

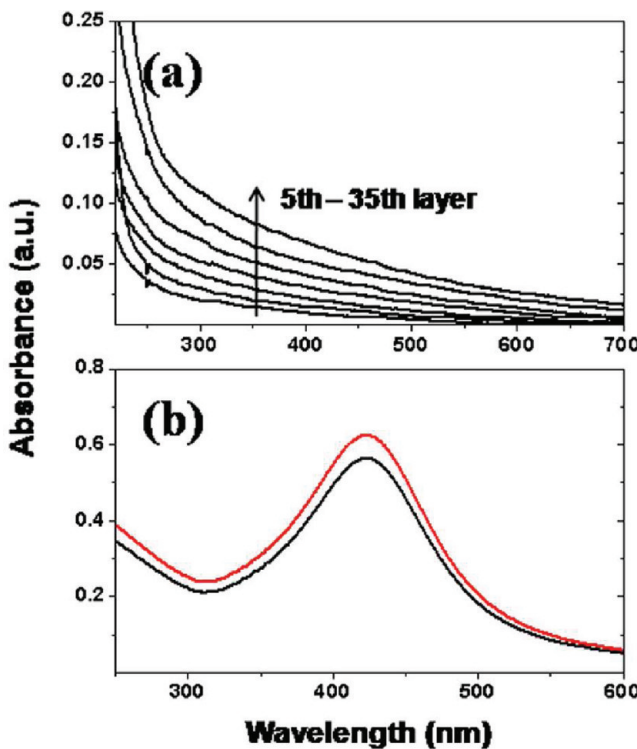


Figure 7. (a) UV-vis absorption spectra showing the growth pattern of multilayer films composed of Q/PAH/(PAA/PEI-Ag⁺)₁₇ before reduction. The UV absorbance was measured at five-layer intervals. (b) UV-vis absorption spectra of the Q/PAH/(PAA/PEI-Ag⁺)₁₇ films after reduction (black line) and after enrichment (red line).

The catalytic performance of both the Q/PAH/(PAA/PEC)₄-Ag(0) and Q/PAH/(PAA/PEC)₄-Ag(0)-en films was investigated. As a model system, the reduction of 4-nitrophenol (4-NPh), which is a toxic material generated from industrial wastewater, to 4-aminophenol (4-APh) was chosen. Usually, 4-NPh in an aqueous solution containing NaBH₄ shows a maximum absorption peak at approximately 400 nm resulting from the formation of 4-nitrophenolate ions.³⁷ In the presence of proper catalysts such as Ag and AuNPs, 4-NPh was reduced to 4-APh and the absorption peak at 400 nm disappeared. However, without suitable catalysts, this reaction does not proceed and the absorption peak remains unaltered for a long time. To examine the catalytic activity of the composite films toward the reduction of 4-NPh, the Q/PAH/(PAA/PEC)₄-Ag(0) and Q/PAH/(PAA/PEC)₄-Ag(0)-en films were immersed in a 4-NPh solution containing NaBH₄ (Figure 8). As the reaction progressed, the absorption peak at 400 nm slowly diminished with the concomitant appearance of a new peak at approximately 300 nm,³⁸ indicating the formation of 4-APh. The reduction of 4-NPh was completed with the complete disappearance of the phenolate peak at 400 nm in 70 min for the Q/PAH/(PAA/PEC)₄-Ag(0) film and in 49 min for the Q/PAH/(PAA/PEC)₄-Ag(0)-en film. This result showed that both of the AgNP-embedded composite films have sufficient catalytic activity to convert 4-NPh to 4-APh, and the Ag-enriched composite film showed a higher catalytic activity than the Q/PAH/(PAA/PEC)₄-Ag(0) film, resulting from the high AgNP content in the composite film matrix.

To investigate the advantages of the film-type catalysts, the catalytic properties were evaluated as a function of pH. Particle-type catalysts, such as AgNP's, showed a relatively good

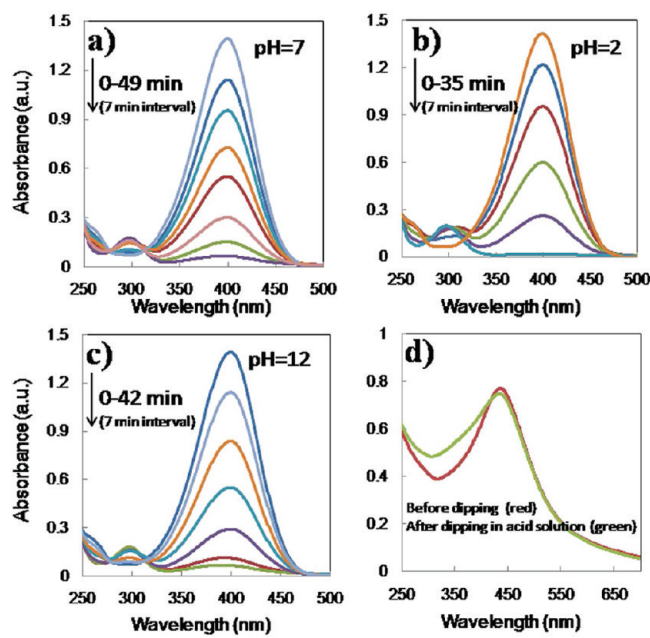


Figure 8. Successive UV-vis spectra of the 4-nitrophenol reduction with NaBH₄ in the presence of the Q/PAH/(PAA/PEC)₄-Ag(0)-en film, which was structurally deformed under (a) pH 7, (b) pH 2, and (c) pH 12. The spectra for the films were recorded at 7 min intervals. (d) UV-vis absorption spectra of the Q/PAH/(PAA/PEC)₄-Ag(0)-en film before (red line) and after (green line) dipping in acid solution (pH 2).

catalytic reaction at neutral pH (Figure S6). However, at low or high pH, the AgNP's agglomerated and precipitated under the harsh conditions because of the instability of the ligands on the surfaces of the AgNP's. Thus, at low or high pH, their catalytic properties were unimpressive. However, a film-type catalyst, the Q/PAH/(PAA/PEC)₄-Ag(0)-en film, showed not only stability but also enhanced catalytic performance at low or high pH (Figure 8a–c). The stability of the Q/PAH/(PAA/PEC)₄-Ag(0)-en film can be attributed to the immobilization of the AgNP's within the composite films as well as the controlled heat treatment of the films. The composite films without heat treatment were damaged at low or high pH, whereas the composite films after heat treatment became robust enough to endure harsh conditions (data not shown). Intensive heat treatment of PEMs consisting of PEI and PAA can induce the transformation of ionic bonding to covalent bonding (imide or amide bond formation between –COO– from PAA and –NH–NH₂ from PEI) and can enhance the mechanical property of the PEM films.³⁹ Under our conditions, covalent bonding was newly formed and ionic bonding was still observed in the films (Figure S7). We believe that the residual ionic bonding induced interesting structural changes in the films and the newly formed covalent bonding enhanced the mechanical property of the films at low or high pH. The enhanced performance of the Q/PAH/(PAA/PEC)₄-Ag(0)-en film can be attributed to structural changes in the film. Surprisingly, the catalytic activity of the PAH/(PAA/PEC)₄-Ag(0)-en film at low or high pH showed a predominant characteristic compared to that at neutral pH, requiring 35 or 42 min to complete the reaction (Figure 8b,c). As expected, the AgNP's are broadly distributed within the swelled PEC structures at low or high pH, whereas they are concentrated within the shrinking PEC structures at neutral pH. At low pH, the carboxylic acid groups

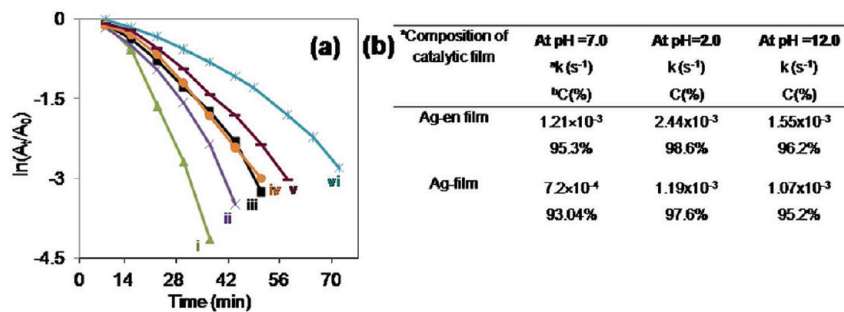


Figure 9. (a) Linear correlation of $\ln(A_t/A_0)$ vs time (where A_t and A_0 stand for absorbance in the intervals and in the initial stage, respectively). (i) Ag-en film (pH 2.0), (ii) Ag-en film (pH 12.0), (iii) Ag-en film (pH 7.0), (iv) Ag film (pH 2.0), (v) Ag film (pH 12.0), and (vi) Ag film (pH 7.0). (b) Calculated rate constants and conversion rates (%) of 4-NPh using Q/PAH/(PAA/PEC)₄-Ag(0) and Q/PAH/(PAA/PEC)₄-Ag(0)-en composite films reduced by NaBH₄ under various pH conditions.

of the PAA are protonated (COOH), whereas the amine groups of the PEI are fully charged (NH_3^+). Consequently, the electrostatic attraction between the PEI and PAA chains decreases markedly, and the electrostatic repulsion between the positive charges (NH_3^+) results in a swelling of the PEC structures. At high pH, the ammonium groups (NH_3^+) of the PEI become fully deprotonated to form NH_2 . Because of the deprotonation of the ammonium groups and the fully charged state of the carboxylic groups of PAA, the negative charges (COO^-) of PAA repel each other, which leads to a swelling of the PEC structures. Thus, the swelled PECs are expected to show enhanced catalytic properties because of the exposure of a large surface area of the AgNP's. Actually, the swelling phenomenon at low and high pH was observed in the Q/PAH/(PAA/PEC)₄-Ag(0)-en film containing the PECs. In an acidic environment, the absorption range of the films containing the PECs was broader compared to that in a neutral environment (Figure 8d). By varying the pH condition, we found that the absorption spectra of the composite films reversibly broadened and narrowed. However, the absorption range of the film without PECs, Q/PAH/(PAA/PEI-Ag(0))₁₇, remained almost unchanged under acidic conditions (Figure S8). As a result, the catalytic activity of this film was unimpressive. These results suggest that the response of the PECs within the films to external stimuli, such as the pH, and their structural changes can enhance their catalytic activity.

The reduction kinetics was monitored by UV-vis absorption spectroscopy of the reaction mixture after the addition of the catalyst. The absorption of 4-NPh at around 400 nm decreases along with a concomitant increase in the peak of 4-APh at around 300 nm (Figures 8 and S9). Because the concentration of BH_4^- added to the mixture is much higher than that of 4-NPh, it is reasonably assumed that the concentration of BH_4^- remains constant during the reaction. In this context, pseudo-first-order kinetics could be used to evaluate the kinetic reaction rate (K) of the current catalytic reaction. As expected, a linear correlation of $\ln(A_t/A_0)$ versus time (where A_t and A_0 stand for absorbance in the intervals and in the initial stage of the 4-nitrophenolate ion, respectively) is obtained. As shown in Figure 9a, the catalytic performance of the Q/PAH/(PAA/PEC)₄-Ag(0)-en films is higher than that of the Q/PAH/(PAA/PEC)₄-Ag(0) film under various pH conditions because of the presence of a high content of AgNP's. At neutral pH, the reaction proceeds comparatively slowly for the both types of films. However, the reaction rate and conversion rate significantly increased in low- and high-pH environments owing to structural changes in the PECs. The calculated rate

constant for the Q/PAH/(PAA/PEC)₄-Ag(0)-en and Q/PAH/(PAA/PEC)₄-Ag(0) films were $1.21 \times 10^{-3} \text{ s}^{-1}$ and $7.2 \times 10^{-4} \text{ s}^{-1}$, respectively. The maximum reaction rate ($2.44 \times 10^{-3} \text{ s}^{-1}$) and conversion rate (98.6%) were obtained by using a Q/PAH/(PAA/PEC)₄-Ag(0)-en film at pH 2 (Figure 9b). Overall, at low pH, both types of films exhibited higher catalytic activities compared to those in high- and neutral-pH environments. Moreover, the catalytic film also showed relatively good recyclable performance (Figure S10). We tested the Q/PAH/(PAA/PEC)₄-Ag(0)-en film at pH 7 after the first use, revealing the stability as well as the reusability of the film. In this case, the time required to complete the reduction of 4-NPh was 63 min (49 min for the first cycle) and the conversion rate was 96.03% ($K = 9.78 \times 10^{-4} \text{ s}^{-1}$).

A major advantage of the composite films is that a large number of NPs can be loaded onto the films, which can significantly enhance the electrical conductivity of the film compared to that of a film prepared by conventional methods. To investigate the electrical properties of our composite films such as Q/PAH/(PAA/PEC)₄-Ag(0) and Q/PAH/(PAA/PEC)₄-Ag(0)-en, a AgNP-embedded conventional PEM film (Q/PAH/(PAA/PEI-Ag(0))₁₇) was prepared for comparison with our composite films. This conventional film was prepared by the layer-by-layer self-assembly method and was used to synthesize AgNP's. However, the conductivity of the conventional Q/PAH/(PAA/PEI-Ag(0))₁₇ film could not be measured because of its extremely high resistivity (Figure S11). The average conductivities of the Q/PAH/(PAA/PEC)₄-Ag(0) and Q/PAH/(PAA/PEC)₄-Ag(0)-en films were measured and found to be 225 and 290 S/cm, respectively. The conductivity of the enriched film, compared to that of the Q/PAH/(PAA/PEC)₄-Ag(0) film, showed an increase of 23%, indicating that there are enough AgNP's within the film to form a conducting network for both composite films and that the enrichment process can further enhance the electrical conductivity of the composite films.

The film-type nanocatalysts synthesized and investigated in this work are very important for the following reasons: (1) they have very well defined PEC nanostructures that are chemically and physically regulated in a systematic, precise, and rapid way; (2) their controlled structures would provide a practically useful platform with structural characteristics and surface functionalities for a variety of applications, as demonstrated in this study; and importantly, (3) this strategy can be easily extended to the fabrication of other film structures undergoing reversible structural changes, which would be applicable in different aspects.

CONCLUSIONS

In this study, a new technique for the fabrication of conductive and catalytic nanocomposite films with a large number of embedded metal NPs was developed that enables the film structure to change reversibly under various pH conditions. Metal NP-enriched nanocomposites films were prepared by the pre- and postadsorption of precursors on PECs within the films, which enhanced the catalytic and electrical properties of the composite films. Thus, this approach can be used as a facile method for preparing conducting composite films and as a new method for producing a film-type catalyst. Because the films contain PECs that are responsive to changes in pH and most of the NPs are embedded in the PECs, interesting catalytic properties, which are unexpected in particle-type catalysts, can be obtained upon changes in the pH. Indeed, as a result of reversible structural changes and the immobilization of NPs within the films, film-type catalysts showed enhanced performance and stability during catalytic reactions under various pH conditions. The results described herein demonstrate the possibility of both a simple process for preparing composite films heavily loaded with metal NPs and a real application for film-type catalysts.

ASSOCIATED CONTENT

Supporting Information

Images of a complex solution. Zeta potential data of PEC-Ag⁺ particles. Growth pattern of Q/PAH/(PAA/PEC-Ag⁺)_n. XPS data of the C 1s core level for the composite film. Catalytic performance of AgNP's. FT-IR data for a composite film before and after heat treatment. Catalytic performance of Q/PAH/(PAA/PEI-Ag(0))₁₇ films. Electrical conductivity of composite films. This material is available free of charge via the Internet at <http://pubs.acs.org>.

AUTHOR INFORMATION

Corresponding Author

^{*}(W.S.C.) E-mail: choiws@hanbat.ac.kr. Fax: +82-42-821-1692.
(H.-J.L.) E-mail: hajinlee@kbsi.re.kr.

Author Contributions

[§]These authors contributed equally to this work.

Notes

The authors declare no competing financial interest.

ACKNOWLEDGMENTS

This work was financially supported by the Korea Basic Science Institute (KBSI, grant T32614), the National Research Foundation of Korea (NRF), the Ministry of Education, Science and Technology (2009-0081966), a grant (code no. 2011-0031639) from the Center for Advanced Soft Electronics under the Global Frontier Research Program of the Ministry of Education Science and Technology, and the intraresearch fund of Hanbat National University (2011).

REFERENCES

- Decher, G. Fuzzy nanoassemblies: toward layered polymeric multicomposites. *Science* **1997**, *277*, 1232–1237.
- Jiang, C.; Tsukruk, V. V. Freestanding nanostructures via layer-by-layer assembly. *Adv. Mater.* **2006**, *18*, 829–840.
- Donath, E.; Sukhorukov, G. B.; Caruso, F.; Davis, S.; Mohwald, H. Novel hollow polymer shells by colloid-templated assembly of polyelectrolytes. *Angew. Chem., Int. Ed.* **1998**, *37*, 2202–2205.
- Shchukin, D. G.; Sukhorukov, G. B.; Mohwald, H. Smart inorganic/organic nanocomposite hollow microcapsules. *Angew. Chem., Int. Ed.* **2003**, *42*, 4472–4475.
- Lee, D.; Rubner, M. F.; Cohen, R. E. Formation of nanoparticle-loaded microcapsules based on hydrogen-bonded multilayers. *Chem. Mater.* **2005**, *17*, 1099–1105.
- Radtchenko, I. L.; Giersig, M.; Sukhorukov, G. B. Inorganic particle synthesis in confined micron-sized polyelectrolyte capsules. *Langmuir* **2002**, *18*, 8204–8208.
- Kidambi, S.; Dai, J.; Li, J.; Bruening, M. L. Selective hydrogenation by Pd nanoparticles embedded in polyelectrolyte multilayers. *J. Am. Chem. Soc.* **2004**, *126*, 2658–2659.
- Choi, W. S.; Yang, H. M.; Koo, H. Y.; Lee, H.-J.; Lee, Y. B.; Bae, T. S.; Jeon, I. C. Smart microcapsules encapsulating reconfigurable carbon nanotube cores. *Adv. Funct. Mater.* **2010**, *20*, 820–825.
- Choi, W. S.; Koo, H. Y.; Kim, D.-Y. Scalable synthesis of chestnut-bur-like magnetic capsules loaded with size-controlled mono- or bimetallic cores. *Adv. Mater.* **2007**, *19*, 451–455.
- Shchukin, D. G.; Sukhorukov, G. B. Nanoparticle synthesis in engineered organic nanoscale reactors. *Adv. Mater.* **2004**, *16*, 671–682.
- Joly, S.; Kane, R.; Radzilowski, L.; Wang, C. T.; Wu, A.; Cohen, R. E.; Thomas, E. L.; Rubner, M. F. Multilayer nanoreactors for metallic and semiconducting particles. *Langmuir* **2000**, *16*, 1354–1359.
- Wang, C. T.; Rubner, M. F.; Cohen, R. E. Polyelectrolyte multilayer nanoreactors for preparing silver nanoparticle composites: controlling metal concentration and nanoparticle size. *Langmuir* **2002**, *18*, 3370–3375.
- Shang, L.; Jin, L.; Guo, S.; Zhai, J.; Dong, S. A facile and controllable strategy to synthesize Au-Ag alloy nanoparticles within polyelectrolyte multilayer nanoreactors upon thermal reduction. *Langmuir* **2010**, *26*, 6713–6719.
- Rahim, M. A.; Nam, B.; Choi, W. S.; Lee, H.-J.; Jeon, I. C. Polyelectrolyte complex particle-based multifunctional freestanding films containing highly loaded bimetallic particles. *J. Mater. Chem.* **2011**, *21*, 11831–11837.
- Tsuchida, E.; Abe, K. Interactions between macromolecules in solution and intermacromolecular complexes. *Adv. Polym. Sci.* **1982**, *45*, 1–119.
- Kabanov, V. A.; Zezin, A. B. Soluble interpolymeric complexes as a new class of synthetic polyelectrolytes. *Pure Appl. Chem.* **1984**, *56*, 343–354.
- Zhang, L.; Li, Y.; Sun, J.; Shen, J. Mechanically stable antireflection and antifogging coatings fabricated by the layer-by-layer deposition process and postcalcination. *Langmuir* **2008**, *24*, 10851–10857.
- Schuetz, P.; Caruso, F. Multilayer thin films based on polyelectrolyte-complex nanoparticles. *Colloids Surf., A* **2002**, *207*, 33–40.
- Zan, X.; Su, Z. Incorporation of nanoparticles into polyelectrolyte multilayers via counterion exchange and in situ reduction. *Langmuir* **2009**, *25*, 12355–12360.
- Dai, J.; Bruening, M. L. Catalytic nanoparticles formed by reduction of metal ions in multilayered polyelectrolyte films. *Nano Lett.* **2002**, *2*, 497–501.
- Belfiore, L. A.; Indra, E. M. Transition metal compatibilization of poly(vinylamine) and poly(ethylene imine). *J. Polym. Sci., Part B* **2000**, *38*, 552–561.
- Glodde, M.; Sirsi, S. R.; Lutz, G. J. Physicochemical properties of low and high molecular weight PEG-grafted poly(ethyleneimine) copolymers and their complexes with oligonucleotides. *Biomacromolecules* **2006**, *7*, 347–356.
- Tan, S.; Erol, M.; Attygalle, A.; Du, H.; Sukhishvili, S. Synthesis of positively charged silver nanoparticles via photoreduction of AgNO₃ in branched poly(ethyleneimine)/HEPES solutions. *Langmuir* **2007**, *23*, 9836–9843.
- Podsiadlo, P.; Paternel, S.; Rouillard, J.-M.; Zhang, Z.; Lee, J.; Lee, J.-W.; Gulari, E.; Kotov, N. A. Layer-by-layer assembly of nacre-

like nanostructured composites with antimicrobial properties. *Langmuir* **2005**, *21*, 11915–11921.

(25) Bohren, C. F.; Huffman, D. R. *Absorption and Scattering of Light by Small Particles*; John Wiley: New York, 1983.

(26) Kreibig, U.; M. Vollmer, M. Optical properties of metal clusters; Springer-Verlag: Berlin, 1995.

(27) Sakata, J. K.; Dwoskin, A. D.; Vigorita, J. L.; Spain, E. M. Film formation of Ag nanoparticles at the organic-aqueous liquid interface. *J. Phys. Chem. B* **2005**, *109*, 138–141.

(28) Cho, J.; Caruso, F. Investigation of the interactions between ligand-stabilized gold nanoparticles and polyelectrolyte multilayer films. *Chem. Mater.* **2005**, *17*, 4547–4553.

(29) Zhang, L.; Sun, J. Layer-by-layer codeposition of polyelectrolyte complexes and free polyelectrolytes for the fabrication of polymeric coatings. *Macromolecules* **2010**, *43*, 2413–2420.

(30) Liu, X.; Dai, B.; Zhou, L.; Sun, J. Polymeric complexes as building blocks for rapid fabrication of layer-by-layer assembled multilayer films and their application as superhydrophobic coatings. *J. Mater. Chem.* **2009**, *19*, 497–504.

(31) King, S. W.; Barnak, J. P.; Bremser, M. D.; Tracy, K. M.; C. Ronning, C.; Davis, R. F.; Nemanich, R. J. Cleaning of AlN and GaN surfaces. *J. Appl. Phys.* **1998**, *84*, 5248–5260.

(32) Hitchcock, A. P.; Urquhart, S. G.; Rightor, E. G. Inner-shell spectroscopy of benzaldehyde, terephthalaldehyde, ethylbenzoate, terephthaloyl chloride and phosgene: models for core excitation of poly(ethylene terephthalate). *J. Phys. Chem.* **1992**, *96*, 8736–8750.

(33) Moulder, J. F.; Stickle, W. F.; Sobol, P. E.; Bomben, K. D. *Handbook of X-ray Photoelectron Spectroscopy*; Perkin-Elmer Corporation: Eden Prairie, MN, 1992.

(34) Kristensen, E. M. E.; Nederberg, F.; Rensmo, H.; Bowden, T.; Hilborn, J.; Siegbahn, H. Photoelectron spectroscopy studies of the functionalization of a silicon surface with a phosphorylcholine-terminated polymer grafted onto (3-aminopropyl)trimethoxysilane. *Langmuir* **2006**, *22*, 9651–9657.

(35) Zielke, U.; Hüttinger, K. J.; Hoffman, W. P. Surface oxidized carbon fibers: II. Chemical modification. *Carbon* **1996**, *34*, 999–1005.

(36) Pamula, E.; Rouxhet, P. G. Bulk and surface chemical functionalities of type III PAN-based carbon fibres. *Carbon* **2003**, *41*, 1905–1915.

(37) Liu, J. C.; Qin, G. W.; Raveendran, P.; Ikushima, Y. Facile “green” synthesis, characterization, and catalytic function of beta-D-glucose-stabilized Au nanocrystals. *Chem.—Eur. J.* **2006**, *12*, 2131–2138.

(38) Ghosh, S. K.; Mandal, M.; Kundu, S.; Nath, S.; Pal, T. Bimetallic Pt–Ni nanoparticles can catalyze reduction of aromatic nitro compounds by sodium borohydride in aqueous solution. *Appl. Catal., A* **2004**, *268*, 61–66.

(39) Balachandra, A. M.; Dai, J.; Bruening, M. L. Enhancing the anion-transport selectivity of multilayer polyelectrolyte membranes by templating with Cu²⁺. *Macromolecules* **2002**, *35*, 3171–3178.